

Opportunistic Wireless Energy Harvesting in Cognitive Radio Networks

Seunghyun Lee, Rui Zhang, *Member, IEEE*, and Kaibin Huang, *Member, IEEE*

Abstract—Wireless networks can be self-sustaining by harvesting energy from ambient *radio-frequency* (RF) signals. Recently, researchers have made progress on designing efficient circuits and devices for RF energy harvesting suitable for low-power wireless applications. Motivated by this and building upon the classic cognitive radio (CR) network model, this paper proposes a novel method for wireless networks coexisting where low-power mobiles in a secondary network, called *secondary transmitters* (STs), harvest ambient RF energy from transmissions by nearby active transmitters in a primary network, called *primary transmitters* (PTs), while opportunistically accessing the spectrum licensed to the primary network. We consider a stochastic-geometry model in which PTs and STs are distributed as independent homogeneous Poisson point processes (HPPPs) and communicate with their intended receivers at fixed distances. Each PT is associated with a *guard zone* to protect its intended receiver from ST's interference, and at the same time delivers RF energy to STs located in its *harvesting zone*. Based on the proposed model, we analyze the transmission probability of STs and the resulting spatial throughput of the secondary network. The optimal transmission power and density of STs are derived for maximizing the secondary network throughput under the given outage-probability constraints in the two coexisting networks, which reveal key insights to the optimal network design. Finally, we show that our analytical result can be generally applied to a non-CR setup, where distributed wireless power chargers are deployed to power coexisting wireless transmitters in a sensor network.

Index Terms—Cognitive radio, energy harvesting, opportunistic spectrum access, wireless power transfer, stochastic geometry.

I. INTRODUCTION

Powering mobile devices by harvesting energy from ambient sources such as solar, wind, and kinetic activities makes wireless networks not only environmentally friendly but also self-sustaining. Particularly, it has been reported in the recent literature that harvesting energy from ambient radio-frequency (RF) signals can power a network of low-power devices such as wireless sensors [1]–[6]. In theory, the maximum power available for RF energy harvesting at a free-space distance of 40 meters is known to be 7 μ W and 1 μ W for 2.4GHz and 900MHz frequency, respectively [2]. Most recently, Zungeru *et al.* have achieved harvested power of 3.5mW at a distance of 0.6 meter and 1 μ W at a distance of 11 meters using Powercast RF energy-harvester operating at

915MHz [2]. It is expected that more advanced technologies for RF energy harvesting will be available in the near future due to e.g. the rapid advancement in designing highly efficient rectifying antennas [3].

In this work, we investigate the impact of RF energy harvesting on the newly emerging cognitive radio (CR) type of networks. To this end, we propose a novel method for wireless networks coexisting where transmitters from a secondary network, called *secondary transmitters* (STs), either opportunistically harvest RF energy from transmissions by nearby transmitters from a primary network, or transmit signals if these *primary transmitters* (PTs) are sufficiently far away. STs store harvested energy in rechargeable batteries with finite capacity and apply the available energy for subsequent transmissions when batteries are fully charged. The throughput of the secondary network is analyzed based on a stochastic-geometry model, where the PTs and STs are distributed according to independent homogeneous Poisson point processes (HPPPs). In this model, each PT is assumed to randomly access the spectrum with a given probability and each active (transmitting) PT is centered at a *guard zone* as well as a *harvesting zone* that is inside the guard zone. As a result, each ST harvests energy if it lies in the harvesting zone of any active PT, or transmits if it is outside the guard zones of all active PTs, or is idle otherwise. This model is applied to maximize the spatial throughput of the secondary network by optimizing key parameters including the ST transmit power and density subject to given PT transmit power and density, guard/harvesting zone radius, and outage-probability constraints in both the primary and secondary networks.

Our work is motivated by a joint investigation of the proposed conventional *opportunistic spectrum access* and the newly introduced *opportunistic energy harvesting* in CR networks, i.e., during the idle time of STs due to the presence of nearby active PTs, they can take such an opportunity to harvest significant RF energy from primary transmissions. Specifically, as shown in Fig. 1, each ST can be in one of the following three modes at any given time: *harvesting mode* if it is inside the harvesting zone of an active PT and not fully charged; *transmitting mode* if it is fully charged and outside the guard zone of all active PTs; and *idle mode* if it is fully charged but inside any of the guard zones, or neither fully charged nor inside any of the harvesting zones.

A. Related Work

Recently, wireless communication powered by energy harvesting has emerged to be a new and active research area.

S. Lee and R. Zhang are with the Department of Electrical and Computer Engineering, National University of Singapore, Singapore (email: {elees, elezhang}@nus.edu.sg). R. Zhang is also with the Institute for Infocomm Research, A*STAR, Singapore.

K. Huang is with the Department of Applied Mathematics, Hong Kong Polytechnic University, Hong Kong (email: huangkb@ieec.org).

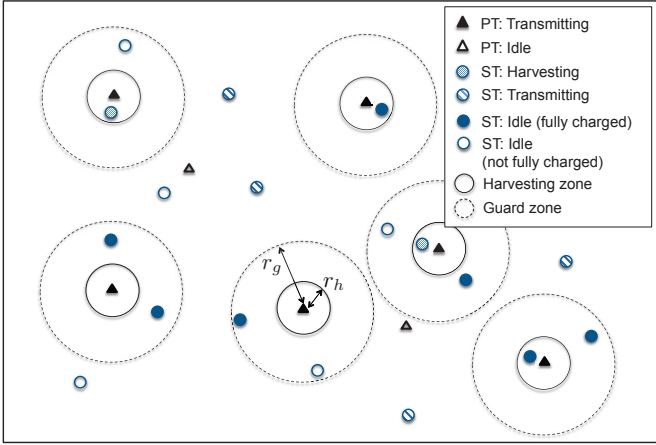


Fig. 1. A wireless energy harvesting CR network in which PTs and STs are distributed as independent HPPPs. Each PT/ST has its intended information receiver at fixed distances (not shown in the figure for brevity). ST harvests energy from a nearby PT if it is inside its harvesting zone. To protect the primary transmissions, ST inside a guard zone is prohibited from transmission.

However, due to energy harvesting, existing transmission algorithms for conventional wireless systems with constant power supplies (e.g., batteries) need to be redesigned to account for the new challenges such as random energy arrivals. For point-to-point wireless systems powered by energy harvesting, the optimal power-allocation algorithms have been designed and shown to follow modified water-filling by Ho and Zhang [7] and Ozel *et al.* [8]. From a network perspective, Huang investigated the throughput of a mobile ad-hoc network (MANET) powered by energy harvesting where the network spatial throughput is maximized by optimizing the transmit power level under an outage constraint [9]. Furthermore, the performance of solar-powered wireless sensor/mesh networks has been analyzed in [10], in which various sleep and wakeup strategies are considered.

Among other energy scavenging sources such as solar and wind, background RF signals can be a viable new source for *wireless energy harvesting* [11]. A new research trend on wireless power transfer is to integrate this technology with wireless communication. In [12] and [13], simultaneous wireless power and information transfer has been investigated, aiming at maximizing information rate and transferred power over single-antenna additive white Gaussian noise (AWGN) channels. For broadcast channels, Zhang and Ho have studied multi-antenna transmission for simultaneous wireless information and power transfer with practical receiver designs such as time switching and power splitting [14]. Moreover, Zhou *et al.* have proposed a new receiver design for enabling wireless information and power transmission at the same time, by judiciously integrating conventional information and energy receivers [15]. For point-to-point wireless systems, Liu *et al.* have studied “opportunistic” RF energy harvesting where the receiver opportunistically harvests RF energy or decodes information subject to time-varying co-channel interference [16]. More recently, Huang and Lau have proposed a new cellular network architecture consisting of power beacons

deployed to deliver wireless energy to mobile terminals and characterized the trade-off between the power-beacon density and cellular network spatial throughput [17].

In another track, the emerging CR technology enables efficient spectrum usage by allowing a secondary network to share the spectrum licensed to a primary network without significantly degrading its performance [18]. Besides active development of algorithms for opportunistic transmissions by secondary users (see e.g. [19], [20] and references therein), notable research has been pursued on characterizing the throughput of coexisting wireless networks based on the tool of stochastic geometry. For example, the capacity trade-offs between two or more coexisting networks sharing a common spectrum have been studied in [21]–[23]. Moreover, the outage probability of a Poisson-distributed CR network with guard zones has been analyzed by Lee and Haenggi [24], where the secondary users opportunistically access the primary users’ channel only when they are not inside any of the guard zones.

B. Summary and Organization

In this paper, we consider a CR network with time slotted transmissions and PT/ST locations modeled by independent HPPPs. The ST transmission power is assumed to be sufficiently small to meet the low-power requirement with RF energy harvesting. Under this setup, the main results of this paper are summarized as follows:

- 1) We propose a new CR network architecture where STs are powered by harvesting RF energy from active primary transmissions. We study the ST transmission probability as a function of ST transmit power in the presence of both guard zones and harvesting zones based on a Markov chain model. For the cases of single-slot and double-slot charging, we obtain the expressions of the exact ST transmission probability, while for the general case of multi-slot charging with more than two slots, we obtain the upper and lower bounds on the ST transmission probability.
- 2) With the result of ST transmission probability, we derive the outage probabilities of coexisting primary and secondary networks subject to their mutual interferences, based on stochastic geometry and a simplified assumption on the HPPP of transmitting STs with an effective density equal to the product of the ST transmission probability and the ST density. Furthermore, we maximize the spatial throughput of the secondary network under given outage constraints for the coexisting networks by jointly optimizing the ST transmission power and density, and obtain simple closed-form expressions of the optimal solution.
- 3) Furthermore, we show that our analytical result can be generally applied to even non-CR setups, where distributed wireless power chargers (WPCs) are deployed to power coexisting wireless information transmitters (WITs) in a sensor network, as shown in Fig. 2. Practically, WPCs can be implemented as e.g. *wireless charging vehicles* [25], or *fixed power beacons* [17] randomly deployed in a wireless sensor network. Based

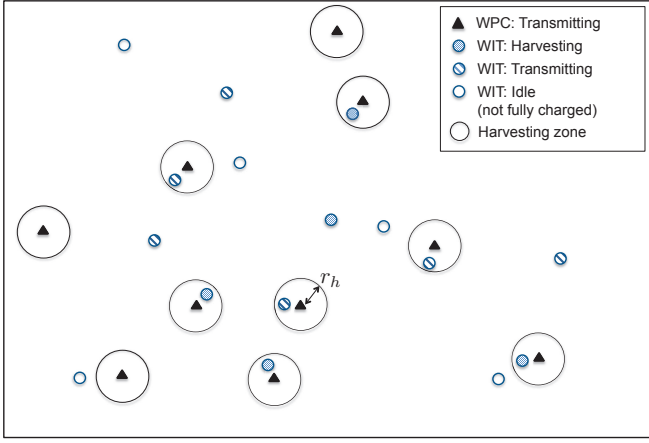


Fig. 2. A wireless powered sensor network in which WPCs and WITs are distributed as independent HPPPs. Each WIT has intended receiver at a fixed distance (not shown in the figure for brevity). WIT harvests energy from a nearby WPC if inside its harvesting zone. Unlike the CR setup in Fig. 1, the guard zone is not applicable in this case, and thus a fully charged WIT can transmit at any time.

on our result for the CR network setup, we derive the maximum network throughput of such wireless powered sensor networks in terms of the optimal density and transmit power of WITs.

The remainder of this paper is organized as follows. Section II describes the system model and performance metric. Section III analyzes the transmission probability of energy-harvesting STs. Section IV studies the outage probabilities in the primary and secondary networks. Section V investigates the maximization of the secondary network throughput subject to the primary and secondary outage probability constraints. Section VI extends the result to the wireless powered sensor network setup. Finally, Section VII concludes the paper.

II. SYSTEM MODEL

A. Network Model

As shown in Fig. 1, we consider a CR network in which PTs and STs are distributed as independent HPPPs¹ with density λ'_p and λ_s , respectively, with $\lambda'_p \ll \lambda_s$. It is assumed that time is slotted and each PT independently accesses the spectrum with probability p at each time slot. Thus, the point process of active PTs forms another HPPP with density $\lambda_p = p\lambda'_p$, according to the Coloring Theorem [28], which varies independently over different slots. For convenience, we refer to active PTs simply as PTs in the rest of this paper. We denote the point processes of PTs and STs as $\Phi_p = \{X\}$ and $\Phi_s = \{Y\}$, respectively, where $X, Y \in \mathbb{R}^2$ denote the coordinates of the PTs and STs, respectively. In addition, it is assumed that each PT/ST transmits with fixed power to its intended primary/secondary receiver (PR/SR) at distances

¹In general, transmitters' locations in cognitive radio networks may have non-homogeneous or even non-Poisson spatial distributions, which are difficult to characterize and not amenable to analysis. In this paper, we assume HPPP for transmitters' locations to obtain tractable analysis for the network performance.

d_p and d_s , respectively, in random directions. We denote the fixed transmission power levels of PTs and STs as P_p and P_s , respectively. We assume $P_p \gg P_s$ in this paper for energy harvesting applications of practical interest.

STs access the spectrum of the primary network and thus their transmissions potentially interfere with PRs. To protect the primary transmissions, STs are prevented from transmitting when they lie in any of the *guard zones*, modeled as disks with a fixed radius centered at each PT. Specifically, let $b(T, x) \subset \mathbb{R}^2$ represent a disk of radius x centered at $T \in \mathbb{R}^2$; then $b(X, r_g)$ denotes the guard zone with radius r_g for protecting PT $X \in \Phi_p$. Define $\mathcal{G} = \bigcup_{X \in \Phi_p} b(X, r_g)$ as the union of all PTs' guard zones; accordingly, an ST $Y \in \Phi_s$ cannot transmit if $Y \in \mathcal{G}$. Note that in practice the guard zone is usually centered at a PR rather than a PT as we have assumed, while our assumption is made to simplify our analysis, similarly as in [19]. We further assume $d_p \ll r_g$ to guarantee that guard zones centered at PTs (rather than PRs) will protect the primary transmissions properly. Under the above assumptions, the probability p_g that a typical ST, denoted by Y^* , does not lie in \mathcal{G} is equal to the probability that there is no PT inside the disk centered at Y^* with radius r_g , i.e., $b(Y^*, r_g)$. Note that the number of PTs inside $b(Y^*, r_g)$, denoted by N , is a Poisson random variable with mean $\pi r_g^2 \lambda_p$; thus, its probability mass function (PMF) is given by

$$\Pr\{N = n\} = e^{-\pi r_g^2 \lambda_p} \frac{(\pi r_g^2 \lambda_p)^n}{n!}, \quad n = 0, 1, 2, \dots \quad (1)$$

Consequently, p_g can be obtained as

$$p_g = \Pr\{Y^* \notin \mathcal{G}\} \quad (2)$$

$$= \Pr\{N = 0\} \quad (3)$$

$$= e^{-\pi r_g^2 \lambda_p}. \quad (4)$$

We assume flat-fading channels with path-loss and Rayleigh fading; hence, the channel gains are modeled as exponential random variables. As a result, in a particular time slot, the signals transmitted from a PT/ST are received at the origin with power $g_X P_p |X|^{-\alpha}$ and $g_Y P_s |Y|^{-\alpha}$, respectively, where $\{g_X\}_{X \in \Phi_p}$ and $\{g_Y\}_{Y \in \Phi_s}$ are independent and identically distributed (i.i.d.) exponential random variables with unit mean, $\alpha > 2$ is the path-loss exponent, and $|X|, |Y|$ denote the distances from node X, Y to the origin, respectively.

B. Energy-Harvesting Model

To make use of the RF energy as an energy-harvesting source, each RF energy harvester in an ST must be equipped with a *power conversion circuit* that can extract DC power from the received electromagnetic waves [1]. Such circuits in practice have certain sensitivity requirements, i.e., the input power needs to be larger than a predesigned threshold for the circuit to harvest RF energy efficiently. This fact thus motivates us to define the *harvesting zone*, which is a disk with radius r_h centered at each PT $X \in \Phi_p$ with $r_h \ll r_g$. The radius r_h is determined by the energy harvesting circuit sensitivity for a given P_p , such that only STs inside a harvesting zone can receive power larger than the energy harvesting threshold, which is given by $P_p r_h^{-\alpha}$. The power received by an ST

outside any harvesting zone is too small to activate the energy harvesting circuit, and thus is assumed to be negligible in this paper.

Let $b(X, r_h)$ represent the harvesting zone centered at PT $X \in \Phi_p$ such that an ST Y can harvest energy from one or more PTs if $Y \in \mathcal{H}$, where $\mathcal{H} = \bigcup_{X \in \Phi_p} b(X, r_h)$ denotes the union of the harvesting zones of all PTs. The probability p_h that a typical ST Y^* lies in \mathcal{H} is equal to the probability that there is at least one PT inside the disk $b(Y^*, r_h)$. Similar to (1), the number of PTs inside $b(Y^*, r_h)$, denoted by K , is a Poisson random variable with mean $\pi r_h^2 \lambda_p$ and PMF given by

$$\Pr\{K = k\} = e^{-\pi r_h^2 \lambda_p} \frac{(\pi r_h^2 \lambda_p)^k}{k!}, \quad k = 0, 1, 2, \dots \quad (5)$$

Accordingly, p_h is given by

$$p_h = \Pr\{Y^* \in \mathcal{H}\} \quad (6)$$

$$= \Pr\{K \geq 1\} \quad (7)$$

$$= \sum_{k=1}^{\infty} e^{-\pi r_h^2 \lambda_p} \frac{(\pi r_h^2 \lambda_p)^k}{k!} \quad (8)$$

$$= 1 - e^{-\pi r_h^2 \lambda_p}. \quad (9)$$

Since λ_p and r_h are both practically small, we can assume $\pi r_h^2 \lambda_p \ll 1$. Thus, p_h given in (8) can be approximated as $\Pr\{K = 1\}$ by ignoring the higher-order terms with $k > 1$. Therefore, when $Y^* \in \mathcal{H}$, Y^* is inside the harvesting zone of one single PT most probably, which equivalently means that the harvesting zones of different PTs do not overlap at most time. As a result, the amount of average power harvested by $Y^* \in \mathcal{H}$ in a time slot can be lower-bounded by $\eta P_p R^{-\alpha}$ where $R \leq r_h$ denotes the distance between Y^* and its nearest PT, and $0 < \eta < 1$ denotes the harvesting efficiency. Note that the harvested power has been averaged over the channel short-term fading within a slot.

C. ST Transmission Model

We assume that each ST has a battery of finite capacity equal to the minimum energy required for one-slot transmission with power P_s for simplicity. Upon the battery being fully charged, an ST will transmit with all stored energy in the next slot if it is outside all the guard zones. We denote the probability that Y^* has been fully charged at the beginning of a time slot as p_f and the probability that it will be able to transmit in this slot as p_t . As mentioned above, the point process of PTs Φ_p varies independently over different slots, and thus the events that an ST has been fully charged in one slot and that it is outside all the guard zones in the next slot are independent. Consequently, p_t can simply be obtained as

$$p_t = p_f p_g, \quad (10)$$

where p_g is given in (4), and p_f will be derived in Section III.

D. Performance Metric

For both PRs and SRs, the received signal-to-interference-plus-noise ratio (SINR) is required to exceed a given target for reliable transmission. Let θ_p and θ_s be the target SINR

for the PR and SR, respectively. The outage probability is then defined as $P_{\text{out}}^{(p)} = \Pr\{\text{SINR}^{(p)} < \theta_p\}$ for the primary network and $P_{\text{out}}^{(s)} = \Pr\{\text{SINR}^{(s)} < \theta_s\}$ for the secondary network. The outage-probability constraints are applied such that $P_{\text{out}}^{(p)} \leq \epsilon_p$ and $P_{\text{out}}^{(s)} \leq \epsilon_s$ with given $0 < \epsilon_p, \epsilon_s < 1$. Note that the transmitting STs in general do not form an HPPP due to the presence of guard zones and energy harvesting zones, but their average density over the network is given by $p_t \lambda_s$. Accordingly, given fixed PT density λ_p and transmission power P_p , the performance metric of the secondary network is the spatial throughput \mathcal{C}_s (bps/Hz/unit-area) given by

$$\mathcal{C}_s = p_t \lambda_s \log_2(1 + \theta_s), \quad (11)$$

under the given primary/secondary outage probability constraints ϵ_p and ϵ_s .

III. TRANSMISSION PROBABILITY OF SECONDARY TRANSMITTERS

In this section, the transmission probability of a typical ST p_t given in (10) is analyzed using the Markov chain model. For convenience, we define M as the maximum number of energy-harvesting time slots required to fully charge the battery of an ST. Since the minimum power harvested by an ST in one slot is $\eta P_p r_h^{-\alpha}$, which occurs when the ST is at the edge of a harvesting zone, it follows that $M = \lceil \frac{P_s}{\eta P_p r_h^{-\alpha}} \rceil$, where $\lceil x \rceil$ denotes the smallest integer larger than or equal to x . Note that $M = 1$ corresponds to the case where the battery is fully charged within one slot time; thus this case is referred to as *single-slot charging*. Similarly, the case of $M = 2$ is referred to as *double-slot charging*. It will be shown in this section that if $M = 1$ or $M = 2$, the battery power level can be exactly modeled by a finite-state Markov chain; hence, the transmission probability p_t can be obtained. However, for *multi-slot charging* with $M > 2$, only upper and lower bounds on p_t are obtained based on the Markov chain analysis for the case of $M = 2$.

A. Single-Slot Charging ($M = 1$)

If $0 < P_s \leq \eta P_p r_h^{-\alpha}$, the battery of an ST is fully charged within a slot, i.e., $M = 1$. It thus follows that the battery power level can only be either 0 or P_s at the beginning of each slot. Consider the finite-state Markov chain with state space $\{0, 1\}$ with states 0 and 1 denoting the battery level of power 0 and P_s , respectively. Furthermore, let \mathbf{P}_1 represent the state-transition probability matrix that can be obtained as

$$\mathbf{P}_1 = \begin{bmatrix} 1 - p_h & p_h \\ p_g & 1 - p_g \end{bmatrix} \quad (12)$$

with p_g and p_h given in (4) and (9), respectively. Then p_t can be obtained by finding the steady-state probability of the assumed Markov chain, as given in the following proposition.

Proposition 3.1: If $0 < P_s \leq \eta P_p r_h^{-\alpha}$ or $M = 1$ (single-slot charging), the transmission probability of a typical ST is

given by

$$p_t = \frac{p_h}{p_h + p_g} p_g \quad (13)$$

$$= \frac{(1 - e^{-\pi r_h^2 \lambda_p}) e^{-\pi r_g^2 \lambda_p}}{1 - e^{-\pi r_h^2 \lambda_p} + e^{-\pi r_g^2 \lambda_p}}. \quad (14)$$

Proof: Let the steady-state probability of the two-state Markov chain be denoted by $\boldsymbol{\pi}_1 = [\pi_{1,0}, \pi_{1,1}]$, where $\boldsymbol{\pi}_1$ is the left eigenvector of \mathbf{P}_1 corresponding to the unit eigenvalue such that

$$\boldsymbol{\pi}_1 \mathbf{P}_1 = \boldsymbol{\pi}_1. \quad (15)$$

From (15), the steady-state distribution of the battery power level at a typical ST is obtained as

$$\pi_{1,0} = \frac{p_g}{p_h + p_g}, \quad \pi_{1,1} = \frac{p_h}{p_h + p_g}. \quad (16)$$

Note that the probability that an ST is fully charged at the beginning of each slot as defined in (10) is $p_f = \pi_{1,1}$ in this case. Consequently, from (10), the desired result in (13) is obtained. ■

It is observed from (14) that in the single-slot charging case, p_t depends only on λ_p , r_h and r_g , but is not related to P_s . The reason is that the battery of an ST is guaranteed to be fully charged over one slot if it gets into a harvesting zone; hence, the probability that an ST is fully charged $p_f = \pi_{1,1} = \frac{p_h}{p_h + p_g}$ does not depend on P_s .

B. Double-Slot Charging ($M = 2$)

If $\eta P_p r_h^{-\alpha} < P_s \leq 2\eta P_p r_h^{-\alpha}$ or $M = 2$, an ST needs at most 2 slots of harvesting to make the battery fully charged. To establish the Markov chain model for this case, we divide the harvesting zone $b(X, r_h)$ into two disjoint regions,

$b(X, h_1)$ and $a(X, h_1, r_h)$, where $h_1 = \left(\frac{P_s}{\eta P_p}\right)^{-\frac{1}{\alpha}} < r_h$ and $a(T, x, y) = b(T, y) \setminus b(T, x)$ denotes the annulus with radii $0 < x < y$ centered at $T \in \mathbb{R}^2$. It then follows that the region $b(X, h_1)$ consists of the locations at which the power harvested by a typical ST Y^* from PT X is greater than or equal to P_s (i.e., single-slot charging region), while the region $a(X, h_1, r_h)$ corresponds to the locations at which the power harvested by Y^* is greater than or equal to $\frac{1}{2}P_s$ but smaller than P_s (see Fig. 3). For convenience, we define $\mathcal{H}_1 = \bigcup_{X \in \Phi_p} b(X, h_1)$ and $\mathcal{H}_2 = \bigcup_{X \in \Phi_p} a(X, h_1, r_h)$. Note that $\mathcal{H} = \mathcal{H}_1 \cup \mathcal{H}_2$. We reasonably assume that \mathcal{H}_1 and \mathcal{H}_2 are disjoint since the harvesting zones are most likely disjoint as mentioned in Section II-B.

Consider a 3-state Markov chain with state space $\{0, 1, 2\}$. Since the battery power level can only be either 0 or in the range $[\frac{1}{2}P_s, P_s]$ since $\eta P_p r_h^{-\alpha} \geq \frac{1}{2}P_s$ in this case, we define state 0 as the battery level of power 0, state 1 with the power level in the range $[\frac{1}{2}P_s, P_s)$, and state 2 with the power level equal to P_s . Note that in order to transit from state 0 to 1, 0 to 2, and 1 to 2, the harvested power at Y^* needs to be $\frac{1}{2}P_s \leq \eta P_p R^{-\alpha} < P_s$, $\eta P_p R^{-\alpha} \geq P_s$, and $\eta P_p R^{-\alpha} \geq \frac{1}{2}P_s$, respectively (or equivalently Y^* needs to be inside \mathcal{H}_2 , \mathcal{H}_1 , and \mathcal{H} , respectively). Thanks to the fact that the minimum charging power is always larger than or equal to $\frac{1}{2}P_s$ in this

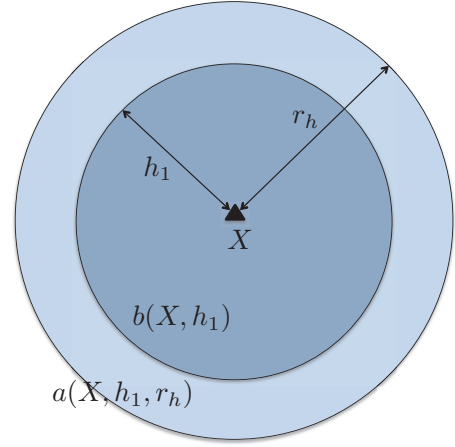


Fig. 3. Divided harvesting zone for the case of double-slot charging ($M = 2$).

case, we can determine the probability of the transition from state 1 to 2, i.e., from the battery power level in the range of $[\frac{1}{2}P_s, P_s)$ to P_s , which occurs when Y^* is (anywhere) inside a harvesting zone (see Fig. 4(a)). Accordingly, the state-transition probability matrix for the assumed 3-state Markov chain (see Fig. 4(b)) is given as

$$\mathbf{P}_2 = \begin{bmatrix} 1 - p_h & p_2 & p_1 \\ 0 & 1 - p_h & p_h \\ p_g & 0 & 1 - p_g \end{bmatrix}, \quad (17)$$

where $p_1 = \Pr\{Y^* \in \mathcal{H}_1\}$ and $p_2 = \Pr\{Y^* \in \mathcal{H}_2\}$. Notice that $p_1 + p_2 = p_h = 1 - e^{-\pi r_h^2 \lambda_p}$, since $\mathcal{H}_1 \cup \mathcal{H}_2 = \mathcal{H}$ and we have assumed that \mathcal{H}_1 and \mathcal{H}_2 are disjoint sets. Similarly to (7), the probability p_1 is given as

$$p_1 = \Pr\{Y^* \in \mathcal{H}_1\} \quad (18)$$

$$= 1 - e^{-\pi h_1^2 \lambda_p}, \quad (19)$$

and p_2 is given as

$$p_2 = p_h - p_1 \quad (20)$$

$$= e^{-\pi h_1^2 \lambda_p} - e^{-\pi r_h^2 \lambda_p}. \quad (21)$$

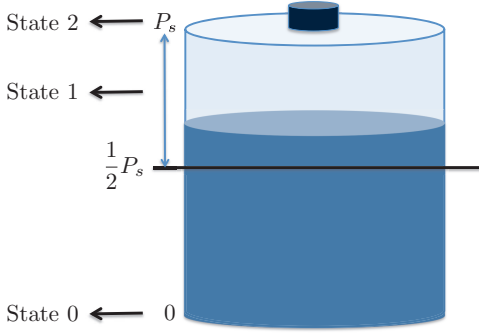
Then we can obtain p_t for this case as given in the following proposition.

Proposition 3.2: If $\eta P_p r_h^{-\alpha} < P_s \leq 2\eta P_p r_h^{-\alpha}$ or $M = 2$ (double-slot charging), the transmission probability of a typical ST is given by

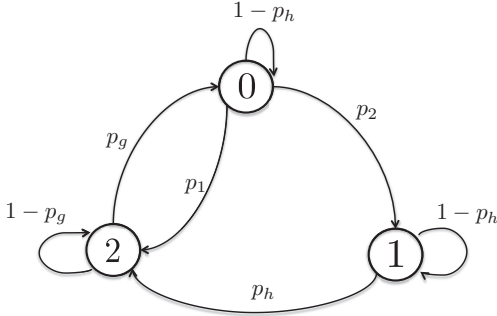
$$p_t = \frac{p_h}{p_h + p_g} p_g \quad (22)$$

$$= \frac{(1 - e^{-\pi r_h^2 \lambda_p}) e^{-\pi r_g^2 \lambda_p}}{1 - e^{-\pi r_h^2 \lambda_p} + e^{-\pi r_g^2 \lambda_p} \left(1 + \frac{e^{-\pi h_1^2 \lambda_p} - e^{-\pi r_h^2 \lambda_p}}{1 - e^{-\pi r_h^2 \lambda_p}}\right)}. \quad (23)$$

Proof: The result in (22) can be obtained by following the similar procedure as in the proof of Proposition 3.1, i.e., by solving $\boldsymbol{\pi}_2 \mathbf{P}_2 = \boldsymbol{\pi}_2$, where $\boldsymbol{\pi}_2$ is the steady-state probability vector given by $\boldsymbol{\pi}_2 = [\pi_{2,0}, \pi_{2,1}, \pi_{2,2}]$. Then, we obtain $p_f = \pi_{2,2}$ and then (22) is obtained from (10). ■



(a) Battery power state of ST



(b) Markov chain model

Fig. 4. The battery power state for the case of $M = 2$ and the corresponding 3-state Markov chain model, where (a) shows an example of the ST being in state 1 of the Markov model in (b), i.e., the current battery power level is in the range $[\frac{1}{2}P_s, P_s)$.

It is worth noting from (23) that p_t in this case is a decreasing function of P_s since $h_1 = \left(\frac{P_s}{\eta P_p}\right)^{-\frac{1}{\alpha}}$ in (23) is such a function. In other words, if P_s increases with fixed P_p and r_h , then the size of $b(X, h_1)$ (single-slot charging region) becomes smaller, which results in an ST harvesting for two slots to be fully charged more frequently, and thus a smaller p_f . Hence, p_t becomes smaller as well given $p_t = p_f p_g$ in (10).

C. Multi-Slot Charging ($M > 2$)

For multi-slot charging with $P_s > 2\eta P_p r_h^{-\alpha}$ or $M > 2$, the minimum charging power at the edge of the harvesting zone, $\eta P_p r_h^{-\alpha}$, is smaller than $\frac{1}{2}P_s$. Unlike the previous two cases of $M = 1$ and $M = 2$, the battery power level in this case cannot be characterized exactly by a finite-state Markov chain since it is not possible in general to uniquely determine the state-transition probabilities.² However, we have shown that for the case of $M = 2$, the battery power level can indeed be characterized with a 3-state Markov chain regardless of the fact that we do not know the exact value of the battery power level in state 1, but rather only know its range $[\frac{1}{2}P_s, P_s)$, provided that the minimum charging power $\eta P_p r_h^{-\alpha}$ is no smaller than

²For instance, if $M = 3$, following the previous two cases, we may divide the battery power level into 4 levels as 0, $[\frac{1}{3}P_s, \frac{2}{3}P_s)$, $[\frac{2}{3}P_s, P_s)$, and P_s and match each level to the states 0, 1, 2, and 3, respectively. Then it can be easily shown that the transition probabilities are unknown for some of the state transitions, e.g., from state 1 to 2.

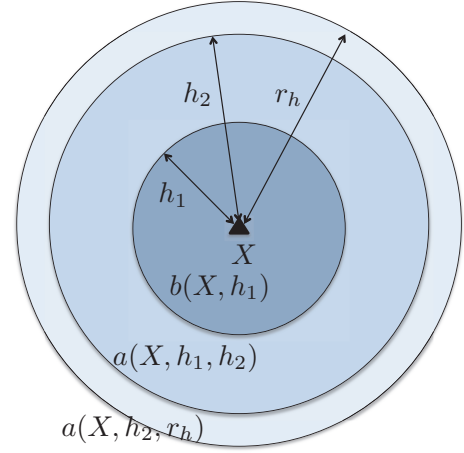


Fig. 5. Divided harvesting zone for the case of $M > 2$. In this case, the amount of power harvested from PT X in $a(X, h_2, r_h)$ is either overestimated as $\frac{1}{2}P_s$ or underestimated as 0 to obtain an upper/lower bound on p_t in Section III-C.

$\frac{1}{2}P_s$. Based on this result, we obtain both the upper and lower bounds on p_t for the case with $M > 2$ as follows.

As shown in Fig. 5, we divide the harvesting zone into 3 disjoint regions $b(X, h_1)$, $a(X, h_1, h_2)$, and $a(X, h_2, r_h)$, where $0 < h_1 < h_2 < r_h$ with h_1 given in the case of $M = 2$ and $h_2 = \left(\frac{P_s}{2\eta P_p}\right)^{-\frac{1}{\alpha}}$. Note that $b(X, h_1)$ is also defined in the case of $M = 2$, while the region $a(X, h_1, h_2)$ consists of the locations in $b(X, r_h)$ at which the power harvested from PT X is larger than or equal to $\frac{1}{2}P_s$, but smaller than P_s , and the region $a(X, h_2, r_h)$ consists of the remaining locations in $b(X, r_h)$ at which the harvested power is smaller than $\frac{1}{2}P_s$. Then, if we assume that the power harvested from a PT in the region $a(X, h_2, r_h)$ is equal to $\frac{1}{2}P_s$ (an overestimation), we can obtain an upper bound on p_t ; however, if we assume it is equal to 0 (an underestimation), we can then obtain a lower bound on p_t , by applying a similar analysis over the 3-state Markov chain as for the case of $M = 2$. For convenience, we define the following mutually exclusive sets $\mathcal{A}_1 = \bigcup_{X \in \Phi_p} b(X, h_1)$, $\mathcal{A}_2 = \bigcup_{X \in \Phi_p} a(X, h_1, h_2)$, and $\mathcal{A}_3 = \bigcup_{X \in \Phi_p} a(X, h_2, r_h)$, where $\mathcal{A}_1 = \mathcal{H}_1$ and $\mathcal{A}_1 \cup \mathcal{A}_2 \cup \mathcal{A}_3 = \mathcal{H}$. Let $p'_2 = \Pr\{Y^* \in \mathcal{A}_2\}$ and $p_3 = \Pr\{Y^* \in \mathcal{A}_3\}$. It then follows that $p_1 + p'_2 + p_3 = p_h$, where p_1 is given in (19) and

$$p'_2 = \Pr\{Y^* \in \mathcal{A}_1 \cup \mathcal{A}_2\} - \Pr\{Y^* \in \mathcal{A}_1\} = e^{-\pi\lambda_p h_1^2} - e^{-\pi\lambda_p h_2^2}, \quad (24)$$

$$p_3 = p_h - p_1 - p'_2 = e^{-\pi\lambda_p h_2^2} - e^{-\pi\lambda_p r_h^2}. \quad (25)$$

The following proposition is then obtained.

Proposition 3.3: If $P_s > 2\eta P_p r_h^{-\alpha}$ or $M > 2$, the transmission probability of an ST is bounded as

$$\frac{p_1 + p'_2}{(p_1 + p'_2) + p_g \left(1 + \frac{p'_2}{p_1 + p_2}\right)} p_g < p_t < \frac{p_h}{p_h + p_g \left(1 + \frac{p'_2 + p_3}{p_h}\right)} p_g. \quad (26)$$

Proof: See Appendix A. \blacksquare

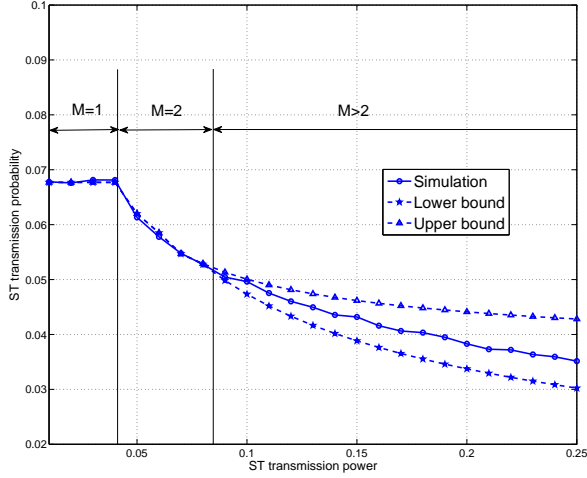


Fig. 6. ST transmission probability p_t versus ST transmission power P_s , with $\lambda_p = 0.01$, $r_g = 4$, $r_h = 1.5$, and $P_p = 2$.

It is worth mentioning that the upper bound on p_t is a decreasing function of P_s since $h_1 = \left(\frac{P_s}{\eta P_p}\right)^{-\frac{1}{\alpha}}$. Also note that the bounds in (26) are tight in the case of $M = 1$ or $M = 2$, since $p'_2 = p_3 = 0$ with $M = 1$, and $p'_2 = p_2$ and $p_3 = 0$ with $M = 2$, thus leading to the same results in (13) and (22), respectively.

Note that unlike the case of $M = 2$, it is not possible to verify in general whether p_t for the case of $M > 2$ is a decreasing function of P_s or not; however, it is conjectured to be so since a larger value of P_s will generally render an ST spend more time to be fully charged. We verify this by simulation in the following subsection (see Fig. 6).

D. Numerical Example

To verify the results on p_t , we provide numerical examples as shown in Figs. 6, 7, and 8. For all of these examples, we set the path-loss exponent as $\alpha = 4$ and the harvesting efficiency as $\eta = 0.1$.

In Fig. 6, we show ST transmission probability p_t versus ST transmission power P_s . It is worth noting that $M = 1$ if $0 < P_s \leq \eta P_p r_h^{-\alpha}$, $M = 2$ if $\eta P_p r_h^{-\alpha} < P_s \leq 2\eta P_p r_h^{-\alpha}$, and $M > 2$ if $P_s > 2\eta P_p r_h^{-\alpha}$. It is observed that p_t is constant if $M = 1$, but is a decreasing function of P_s if $M = 2$, which agrees with the results in (14) and (23), respectively. It is also shown that if $M > 2$, p_t is still a decreasing function of P_s as we conjectured. Moreover, the upper bound and lower bound on p_t obtained in (26) for $M > 2$ are depicted in this figure. These bounds are observed to be tight when $M = 1$ and $M = 2$, while they get looser with increasing P_s when $M > 2$. The reason is that the size of the region $a(X, h_2, r_h)$ shown in Fig. 5, in which we overestimate or underestimate the harvested power, enlarges with increasing P_s . However, since only small value of P_s is of our interest, we can assume that these bounds are reasonably accurate for small values of M .

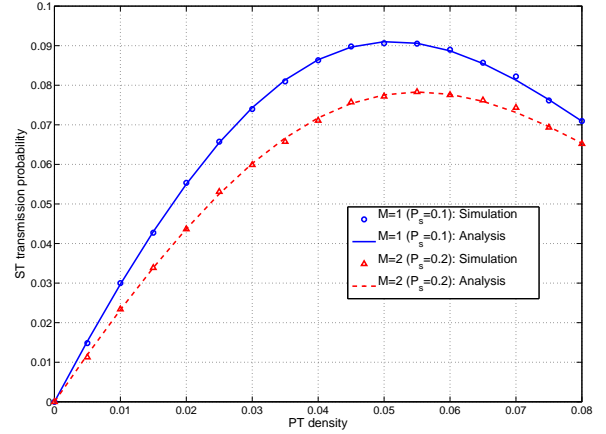


Fig. 7. ST transmission probability p_t versus PT density λ_p , with $r_g = 3$, $r_h = 1$ and $P_p = 1$.

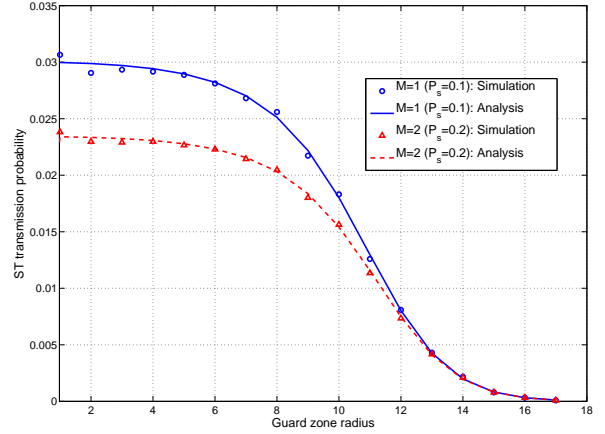


Fig. 8. ST transmission probability p_t versus the radius of guard zone r_g , with $\lambda_p = 0.01$, $r_h = 1$, and $P_p = 1$.

Fig. 7 shows p_t versus PT density λ_p . It is observed that for both $M = 1$ and $M = 2$, p_t first increases with λ_p when λ_p is small but starts to decrease with λ_p when λ_p becomes sufficiently large. This can be explained as follows. If λ_p is small, increasing λ_p is more beneficial since each ST will get charged more frequently and thus be able to transmit (i.e., p_f increases more substantially than the decrease of p_g). However, after λ_p exceeds a certain threshold, increasing λ_p will more pronounce the effect of guard zones and thus make STs transmit less frequently (i.e., p_g decreases more substantially than the increase of p_f).

In Fig. 8, we show p_t versus the guard zone radius r_g . It is observed that p_t is a decreasing function of r_g . Intuitively, this result is expected since larger r_g results in STs transmitting less frequently, i.e., smaller values of p_g , and it is known from (10) that $p_t = p_f p_g$.

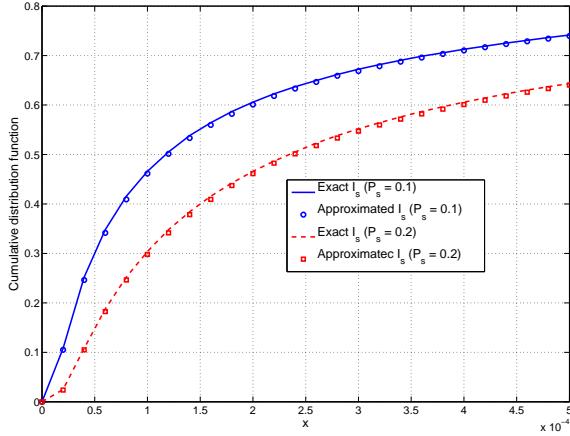


Fig. 9. The CDF of exact I_s and approximated I_s (based on Assumption 1) with $\alpha = 4$, $\eta = 0.1$, $r_g = 3$, $r_h = 1$, $\lambda_s = 0.2$, $\lambda_p = 0.01$, and $P_p = 2$.

IV. OUTAGE PROBABILITY

In this section, the outage probabilities of both the primary and secondary networks are studied. Let Φ_t denote the point process of the active (transmitting) STs. In addition, let I_p and I_s indicate the aggregate interference at the origin from all PTs and active STs, respectively, which are modeled by *shot-noise processes* [28], given by $I_p = \sum_{X \in \Phi_p} g_X P_p |X|^{-\alpha}$ and $I_s = \sum_{Y \in \Phi_t} g_Y P_s |Y|^{-\alpha}$, respectively. Note that in general, due to the presence of the guard zone and/or harvesting zone, in each time slot, the point process Φ_t is not necessarily an HPPP; thus, I_s is not the shot-noise process of an HPPP. Accordingly, the outage probabilities $P_{\text{out}}^{(p)}$ and $P_{\text{out}}^{(s)}$ for primary and secondary networks, both related to I_s , are difficult to be characterized exactly. To overcome this difficulty, we make the following assumption on the process of active STs.

Assumption 1: The point process of active STs Φ_t is an HPPP with density $p_t \lambda_s$.

It is shown in Fig. 9 that the cumulative distribution function (CDF) of I_s , given by $\Pr\{I_s \leq x\}$, obtained by simulations, can be well approximated by that of approximated I_s based on Assumption 1. Further verifications of Assumption 1 will be given later by simulations (see Figs. 11 and 12).

Let $\Lambda(\lambda)$ denote the HPPP with density $\lambda > 0$. Under Assumption 1, the distribution of Φ_t is the same as that of $\Lambda(p_t \lambda_s)$. It thus follows that I_s can be rewritten as

$$I_s = \sum_{Y \in \Lambda(p_t \lambda_s)} g_Y P_s |Y|^{-\alpha}. \quad (27)$$

Consider first the outage probability of the primary network, $P_{\text{out}}^{(p)}$, which can be characterized by considering a typical PR located at the origin. Slivnyak's theorem [28] states that an additional PT corresponding to the PR at the origin does not affect the distribution of Φ_p . Therefore, the outage probability of the PR at the origin is expressed as

$$P_{\text{out}}^{(p)} = \Pr \left\{ \frac{g_p P_p d_p^{-\alpha}}{I_p + I_s + \sigma^2} < \theta_p \right\}, \quad (28)$$

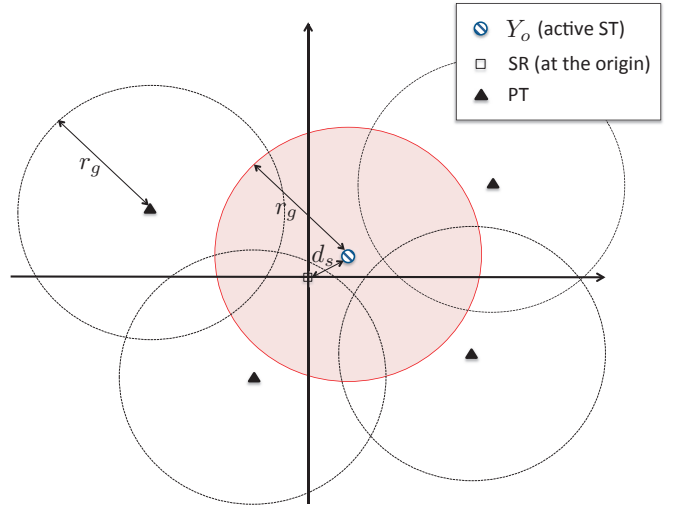


Fig. 10. A typical SR located at the origin, for which there is no PT inside the shaded region $b(Y_o, r_g)$.

where g_p is the channel power between the PR at the origin and its corresponding PT, and σ^2 is the AWGN power. Then, $P_{\text{out}}^{(p)}$ is obtained in the following lemma.

Lemma 4.1: Under Assumption 1, the outage probability of a typical PR at the origin is given by

$$P_{\text{out}}^{(p)} = 1 - \exp(-\tau_p), \quad (29)$$

where

$$\tau_p = \left(\lambda_p + p_t \lambda_s \left(\frac{P_s}{P_p} \right)^{\frac{\alpha}{2}} \right) \theta_p^{\frac{2}{\alpha}} d_p^2 \varphi + \frac{\theta_p d_p^\alpha \sigma^2}{P_p}, \quad (30)$$

$\varphi = \pi \frac{2}{\alpha} \Gamma(\frac{2}{\alpha}) \Gamma(1 - \frac{2}{\alpha})$, with $\Gamma(x) = \int_0^\infty y^{x-1} e^{-y} dy$ denoting the Gamma function.

Proof: See Appendix B. ■

Next, consider the outage probability of the secondary network, $P_{\text{out}}^{(s)}$, which can be characterized by a typical SR located at the origin. Note that there must be an active ST, denoted by Y_o , corresponding to the SR at the origin. Since an ST cannot transmit if it is inside any guard zone, to accurately approximate $P_{\text{out}}^{(s)}$ under Assumption 1, we consider the outage probability conditioned on that Y_o is outside all the guard zones and thus there is no PT inside the disk of radius r_g centered at Y_o (see Fig. 10). Let the event in the above condition be denoted by $\mathcal{E} = \{\Phi_p \cap b(Y_o, r_g) = \emptyset\}$. Then the outage probability of a typical SR at the origin can be obtained as

$$P_{\text{out}}^{(s)} = \Pr \left\{ \frac{g_s P_s d_s^{-\alpha}}{I_p + I_s + \sigma^2} < \theta_s \mid \mathcal{E} \right\}, \quad (31)$$

where g_s is the channel power between the SR at the origin and the corresponding ST Y_o . From the law of total probability we have

$$P_{\text{out}}^{(s)} = \frac{\Pr \left\{ \frac{g_s P_s d_s^{-\alpha}}{I_p + I_s + \sigma^2} < \theta_s \right\} - \Pr \left\{ \frac{g_s P_s d_s^{-\alpha}}{I_p + I_s + \sigma^2} < \theta_s \mid \bar{\mathcal{E}} \right\} \Pr\{\bar{\mathcal{E}}\}}{\Pr\{\mathcal{E}\}}. \quad (32)$$

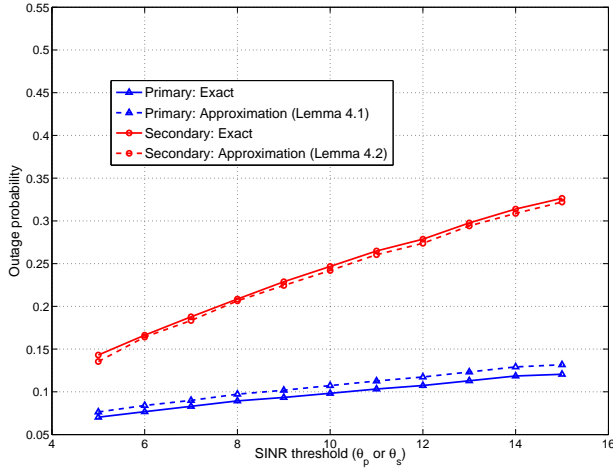


Fig. 11. Outage probability of primary and secondary network versus SINR threshold, with $\alpha = 4$, $\eta = 0.1$, $d_p = d_s = 0.5$, $r_g = 3$, $r_h = 1$, $\lambda_p = 0.01$, $\lambda_s = 0.1$, $P_p = 1$, and $P_s = 0.1$.

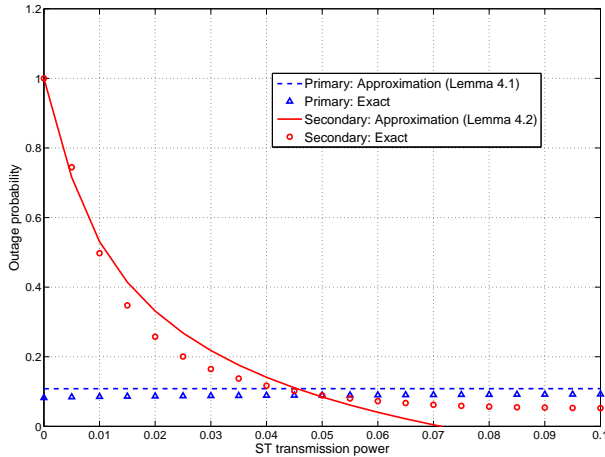


Fig. 12. Outage probability of primary and secondary network versus ST transmission power P_s , with $\alpha = 4$, $\eta = 0.1$, $d_p = d_s = 0.5$, $r_g = 4$, $r_h = 1$, $\lambda_s = 0.2$, $\lambda_p = 0.01$, $\theta_p = \theta_s = 5$, and $P_p = 2$.

Note that $\bar{\mathcal{E}} = \{\Phi_p \cap b(Y_o, r_g) \neq \emptyset\}$. Then we have the following lemma.

Lemma 4.2: Under Assumption 1, the outage probability of the typical SR at the origin is approximated by

$$P_{\text{out}}^{(s)} \approx \frac{1 - \exp(-\tau_s) - (1 - p_g)}{p_g}, \quad (33)$$

where

$$\tau_s = \left(\lambda_p \left(\frac{P_s}{P_p} \right)^{-\frac{2}{\alpha}} + p_t \lambda_s \right) \theta_s^{\frac{2}{\alpha}} d_s^2 \varphi + \frac{\theta_s d_s^\alpha \sigma^2}{P_s}. \quad (34)$$

Proof: See Appendix C. ■

Although I_s can be well approximated by (27) based on Assumption 1, it is worth mentioning that the approximated result of $P_{\text{out}}^{(p)}$ and $P_{\text{out}}^{(s)}$ in Lemmas 4.1 and 4.2, respectively,

are valid only when $P_p \gg P_s$, as assumed in this paper for the following reasons. First, to derive $P_{\text{out}}^{(p)}$ under Assumption 1, STs are uniformly located and thus can be inside the guard zone corresponding to the typical PR at the origin, and as a result cause interference to the PR. However, if we assume $P_p \gg P_s$, the interference due to STs inside this guard zone is negligible and thus can be ignored. Next, to derive $P_{\text{out}}^{(s)}$, as shown in Appendix C, the term $\Pr \left\{ \frac{g_s P_s d_s^{-\alpha}}{I_p + I_s + \sigma^2} < \theta_s \mid \bar{\mathcal{E}} \right\}$ in (32) can be assumed to be 1 only when $P_p \gg P_s$. In Figs. 11 and 12, we compare the outage probabilities obtained by simulations and those based on the approximations in (29) and (33). It is observed that our approximations are quite accurate and thus Assumption 1 is validated.

In addition, it can be inferred from (33) and (34) that $P_{\text{out}}^{(s)}$ is in general a decreasing function of P_s , since τ_s is a decreasing function of P_s . This implies that large ST transmission power P_s is beneficial to reducing the secondary network outage probability, although larger P_s also increases the interference level from other active STs. This can be explained by the fact that if P_s is increased, the increase of received signal power by the SR at the origin can be shown to be more significant than the increase of interference power from all other active STs. On the other hand, from (29) and (30), it is analytically difficult to show whether $P_{\text{out}}^{(p)}$ is a decreasing or increasing function of P_s . This is because in general there is a trade-off for setting P_s to minimize the primary outage probability, since larger P_s increases the interference level from active STs (resulting in larger $P_{\text{out}}^{(p)}$) but at the same time reduces the ST transmission probability p_t (see Fig. 6) and thus the number of active STs (resulting in smaller $P_{\text{out}}^{(p)}$). In Fig. 12, we show the outage probabilities $P_{\text{out}}^{(p)}$ and $P_{\text{out}}^{(s)}$ versus P_s , respectively. It is observed that $P_{\text{out}}^{(s)}$ is a decreasing function of P_s , whereas $P_{\text{out}}^{(p)}$ is quite insensitive to the change of P_s .

V. NETWORK THROUGHPUT MAXIMIZATION

In this section, the spatial throughput of the secondary network defined in (11) is investigated under the primary and secondary outage constraints. To be more specific, with fixed P_p , λ_p , r_g , and r_h , the throughput of the secondary network \mathcal{C}_s is maximized over P_s and λ_s under given ϵ_p and ϵ_s . The optimization problem can thus be formulated as follows.

$$(P1) : \max_{P_s, \lambda_s} p_t \lambda_s \log_2(1 + \theta_s) \quad (35)$$

$$\text{s.t. } P_{\text{out}}^{(p)} \leq \epsilon_p \quad (36)$$

$$P_{\text{out}}^{(s)} \leq \epsilon_s, \quad (37)$$

where $P_{\text{out}}^{(p)}$ and $P_{\text{out}}^{(s)}$ are given by (29) and (33), respectively. With other parameters being fixed, the transmission probability p_t is in general a function of P_s (cf. Section III). Thus, we denote p_t as $p_t(P_s)$ in the sequel.

Since $\log_2(1 + \theta_s)$ in (35) is a constant and $P_{\text{out}}^{(p)}$, $P_{\text{out}}^{(s)}$ are monotonically increasing functions of τ_p and τ_s , respectively

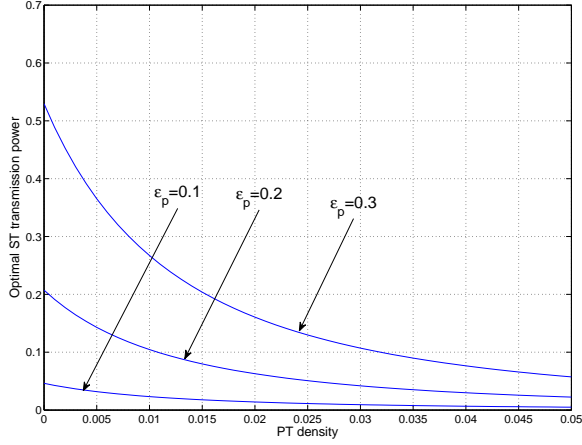


Fig. 13. Optimal ST transmission power P_s^* versus PT density λ_p , with $\alpha = 4$, $d_p = d_s = 0.5$, $r_h = 1$, $r_g = 3$, $P_p = 2$, $\epsilon_s = 0.3$, and $\theta_p = \theta_s = 5$.

(see (29) and (33)), (P1) is equivalently expressed as

$$\max_{P_s, \lambda_s} p_t(P_s)\lambda_s \quad (38)$$

$$\text{s.t. } \tau_p \leq \mu_p \quad (39)$$

$$\tau_s \leq \mu_s, \quad (40)$$

where $\mu_p = -\ln(1 - \epsilon_p)$ and $\mu_s = -\ln((1 - \epsilon_s)p_g)$. Note that μ_p and μ_s are increasing functions of ϵ_p and ϵ_s , respectively. In general, it is challenging to find a closed-form solution for (38) with $\sigma^2 > 0$. However, if we assume that the network is primarily interference-limited, by setting $\sigma^2 = 0$, a closed-form solution for (P1) can be obtained as given in the following theorem.

Theorem 5.1: Assuming $\sigma^2 = 0$, the maximum throughput of the secondary network is given by

$$C_s^* = \frac{\mu_s(\mu_p - \varphi\theta_p^{\frac{2}{\alpha}}d_p^2\lambda_p)}{\theta_s^{\frac{2}{\alpha}}d_s^2\mu_p\varphi} \log_2(1 + \theta_s), \quad (41)$$

where the optimal ST transmit power is

$$P_s^* = \frac{\theta_s}{\theta_p} \left(\frac{d_s}{d_p}\right)^\alpha \left(\frac{\mu_s}{\mu_p}\right)^{-\frac{\alpha}{2}} P_p, \quad (42)$$

and the optimal ST density is

$$\lambda_s^* = \frac{\mu_s(\mu_p - \varphi\theta_p^{\frac{2}{\alpha}}d_p^2\lambda_p)}{p_t(P_s^*)\theta_s^{\frac{2}{\alpha}}d_s^2\mu_p\varphi}. \quad (43)$$

Proof: See Appendix D. ■

Note that since $p_t(P_s^*)$ has been obtained in close-form for the case of $0 < P_s^* \leq 2\eta P_p r_h^{-\alpha}$ (i.e., $M = 1$ or $M = 2$ in Section III), the optimal ST density λ_s^* in (43) can be obtained exactly for this case, according to (14) and (23). Otherwise, only upper and lower bounds on λ_s^* can be obtained, based on (26).

Some remarks are in order.

- It is worth noting that $\mu_s = -\ln((1 - \epsilon_s)p_g)$ in (40) is an increasing function of PT density λ_p , since p_g given

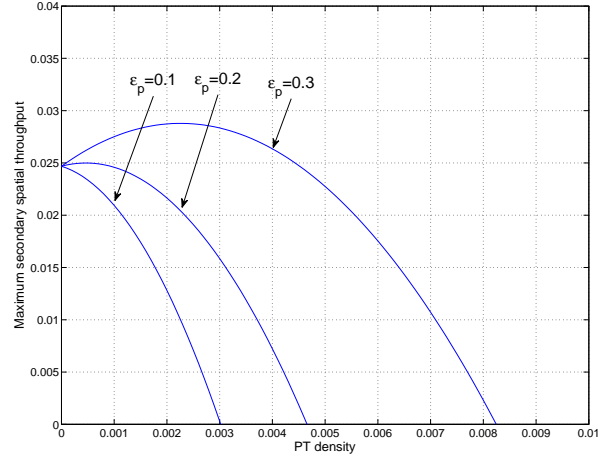


Fig. 14. Maximum secondary spatial throughput C_s^* versus PT density λ_p , with $\alpha = 4$, $d_p = d_s = 0.5$, $r_h = 1$, $r_g = 3$, $P_p = 2$, $\epsilon_s = 0.3$, and $\theta_p = \theta_s = 5$.

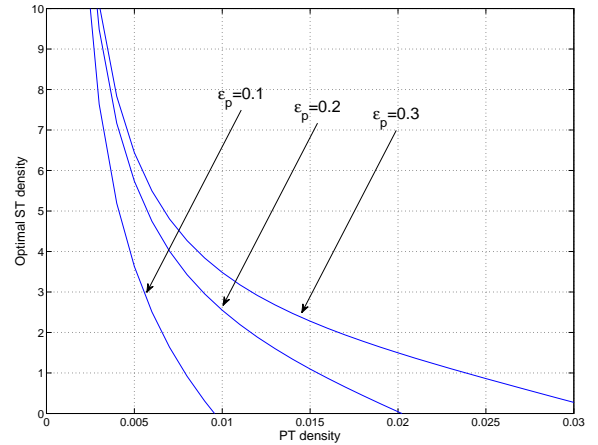


Fig. 15. Optimal ST density λ_s^* versus PT density λ_p , with $\alpha = 4$, $d_p = d_s = 0.5$, $r_h = 1$, $r_g = 3$, $P_p = 2$, $\epsilon_s = 0.3$, and $\theta_p = \theta_s = 5$.

in (4) is a decreasing function of λ_p . Hence, the optimal ST transmission power P_s^* given in (42) decreases with increasing λ_p . This result is shown in Fig. 13, with three different values of ϵ_p .

- In Fig. 14, we show the maximum secondary spatial throughput C_s^* given in (41) versus λ_p with $\epsilon_p = 0.1$, 0.2, or 0.3. Note that from the perspective of RF energy harvesting, larger λ_p is beneficial to the secondary network throughput. However, it is observed that if $\epsilon_p = 0.1$, C_s^* decreases with λ_p , while for $\epsilon_p = 0.2$ or 0.3, C_s^* first increases with λ_p when λ_p is small but eventually starts to decrease when λ_p exceeds a certain threshold. The reason of this phenomenon can be explained as follows. When ϵ_p is small as compared with ϵ_s (e.g., $\epsilon_p = 0.1$ in Fig. 14), the constraint in (39) prevails over that in (40), i.e., satisfying (39) is sufficient to satisfy (40), but not vice versa. Therefore, in this case, if λ_p is increased,

the active STs' density $p_t \lambda_s$ or C_s^* will be decreased to reduce τ_p in (39), i.e., reducing the network interference level. However, when ϵ_p is relatively larger (e.g., $\epsilon_p = 0.2$ or 0.3 in Fig. 14), (40) prevails over (39). As a result, if λ_p is increased, then so is μ_s in (40), and thus $p_t \lambda_s$ or C_s^* will be increased. However, if λ_p exceeds a certain threshold, $p_t \lambda_s$ will be decreased to reduce τ_s in (40); as a result, C_s^* decreases with increasing λ_p .

- It is revealed from (43) that for given λ_p , the optimal active STs' density $p_t(P_s^*)\lambda_s^*$ is fixed under a given pair of primary and secondary outage constraints. In other words, λ_s^* is inversely proportional to $p_t(P_s^*)$. This implies that as p_t converges to zero with $\lambda_p \rightarrow 0$ (see Fig. 7), λ_s^* diverges to infinity at the same time, as shown in Fig. 15. Thus, although the sparse PT density will lead to larger secondary network throughput (see Fig. 14), a correspondingly large number of STs need to be deployed to achieve the maximum throughput, each with a very small transmission probability p_t . As a result, only a small fraction of the STs could be active at any time, resulting in large delay for secondary transmissions or inefficient secondary network design.

VI. APPLICATION AND EXTENSION

In this section, we extend our results on the CR network to the application scenario depicted in Fig. 2, where a set of distributed wireless power chargers (WPCs) are deployed to power wireless information transmitters (WITs) in a sensor network. It is assumed that wireless power transmission from WPCs to WITs is over a dedicated band which is different from that for the information transfer, and thus does not interfere with wireless information receivers (WIRs). For simplicity, we assume that the path-loss exponents for both the power transmission and information transmission are equal to α . Moreover, the network models for WPCs and WITs as well as the energy harvesting and transmission models of WITs are similarly assumed as in Section II for PTs and STs in the CR setup. For convenience, we thus use the same symbol notations for PTs and STs to represent for WPCs and WITs, respectively.

A. Transmission Probability

Unlike the CR case, WITs in a sensor network do not need to be prevented from transmissions by guard zones, since there are no PTs present. As a result, a WIT can transmit at any time provided that it is fully charged. By letting $r_g = 0$, we have $p_g = 1$, and from (14), (23) and (26) we obtain the transmission probability of a typical WIT in the following corollary.

Corollary 6.1: The transmission probability of a typical WIT is given by

- 1) If $0 < P_s \leq \eta P_p r_h^{-\alpha}$ or $M = 1$,

$$p_t = \frac{p_h}{1 + p_h}. \quad (44)$$

- 2) If $\eta P_p r_h^{-\alpha} < P_s \leq 2\eta P_p r_h^{-\alpha}$ or $M = 2$,

$$p_t = \frac{p_h}{p_h + 1 + \frac{p_2'}{p_h}}. \quad (45)$$

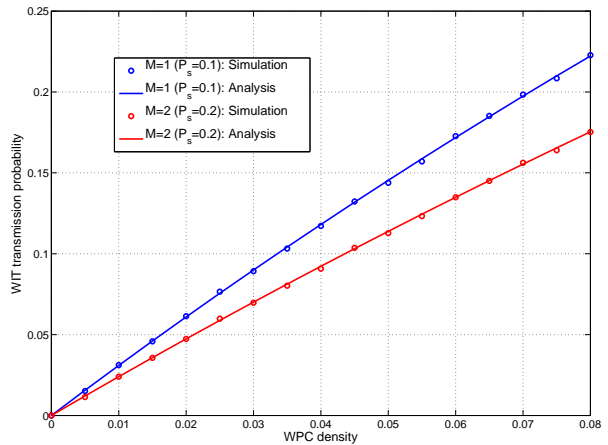


Fig. 16. WIT transmission probability p_t versus WPC density λ_p , with $\alpha = 4$, $\eta = 0.1$, $r_h = 1$, $r_g = 3$, and $P_p = 1$.

- 3) If $P_s > 2\eta P_p r_h^{-\alpha}$ or $M > 2$,

$$\frac{p_1 + p_2'}{p_1 + p_2' + 1 + \frac{p_2'}{p_1 + p_2'}} \leq p_t \leq \frac{p_h}{p_h + 1 + \frac{p_2' + p_3}{p_h}}, \quad (46)$$

where $p_h = 1 - e^{-\pi r_h^2 \lambda_p}$ is given in (9); $p_1 = 1 - e^{-\pi h_1^2 \lambda_p}$ and $p_2 = e^{-\pi h_1^2 \lambda_p} - e^{-\pi r_h^2 \lambda_p}$ are given in (19) and (21), respectively; $p_2' = e^{-\pi \lambda_p h_1^2} - e^{-\pi \lambda_p h_2^2}$ and $p_3 = e^{-\pi \lambda_p h_2^2} - e^{-\pi \lambda_p r_h^2}$ are given in (24) and (25), respectively.

It is worth noting that unlike the CR setup, p_t in this case is in general an increasing function of λ_p since there are no guard zones and thus larger λ_p always help charge WITs more frequently, as shown in Fig. 16.

B. Network Throughput Maximization

Note that unlike the CR setup, here we only need to consider the outage probability of a typical WIR at the origin due to the interference of other active WITs. Similar to Assumption 1, we assume that active WITs form an HPPP with density $p_t \lambda_s$; thus, the outage probability of a typical WIR at the origin can be obtained by simplifying Lemma 4.1 as

$$P_{\text{out}}^{(s)} = \Pr \left\{ \frac{g_s P_s d_s^{-\alpha}}{I_s + \sigma^2} < \theta_s \right\} \quad (47)$$

$$= 1 - \exp(-\tau_s), \quad (48)$$

where in this case τ_s is given by

$$\tau_s = \theta_s^{\frac{2}{\alpha}} d_s^2 \varphi p_t \lambda_s + \frac{\theta_s d_s^\alpha \sigma^2}{P_s}. \quad (49)$$

For the sensor network throughput maximization, Problem (P1) can be modified such that only the outage constraint for the WIR is applied. Thus we have the following simplified problem.

$$(P2): \max_{P_s, \lambda_s} p_t(P_s) \lambda_s \log_2(1 + \theta_s) \quad (50)$$

$$\text{s.t. } P_{\text{out}}^{(s)} \leq \epsilon_s. \quad (51)$$

The solution of (P2) is given in the following corollary, based on Theorem 5.1.

Corollary 6.2: Assuming $\sigma^2 = 0$, the maximum network throughput is given by

$$C_s^* = \frac{\mu'_s}{\theta_s^\alpha d_s^2 \varphi} \log_2(1 + \theta_s), \quad (52)$$

where $\mu'_s = -\ln(1 - \epsilon_s)$, and the optimal solution $(P_s^*, \lambda_s^*) \in \mathbb{R}_+ \times \mathbb{R}_+$ is any pair satisfying

$$p_t(P_s^*)\lambda_s^* = \frac{\mu'_s}{\theta_s^\alpha d_s^2 \varphi}. \quad (53)$$

Proof: With $\sigma^2 = 0$, from (48) and (49), Problem (P2) can be equivalently rewritten as

$$\max_{P_s, \lambda_s} p_t(P_s)\lambda_s \quad (54)$$

$$\text{s.t. } p_t(P_s)\lambda_s \leq \frac{\mu'_s}{\theta_s^\alpha d_s^2 \varphi}, \quad (55)$$

where $\mu'_s = -\ln(1 - \epsilon_s)$. To maximize $p_t(P_s)\lambda_s$, then it is easy to see from (55) that the optimal solution is $p_t(P_s^*)\lambda_s^* = \frac{\mu'_s}{\theta_s^\alpha d_s^2 \varphi}$; by multiplying it with $\log_2(1 + \theta_s)$, we then obtain C_s^* in (52). \blacksquare

Note that unlike the result in Theorem 5.1, the maximum network throughput remains constant regardless of λ_p . This is because there is no primary outage constraint in this case and thus the optimal density of active WITs $p_t(P_s^*)\lambda_s^*$ is determined solely by the outage constraint of WIRs. On the other hand, if λ_p is increased, we can effectively reduce the required WIT density λ_s^* for achieving the same C_s^* since p_t in general increases with λ_p .

VII. CONCLUSION

In this paper, we have proposed a novel network architecture enabling secondary users to harvest energy as well as reuse the spectrum of primary users in the CR network. Based on stochastic-geometry models and certain assumptions, our study revealed useful insights to optimally design the RF energy powered CR network. We derived the transmission probability of a secondary transmitter by considering the effects of both the guard zones and harvesting zones, and thereby characterized the maximum secondary network throughput under the given outage constraints for primary and secondary users, and the corresponding optimal secondary transmit power and transmitter density in closed-form. Moreover, we showed that our result can also be applied to the wireless sensor network powered by a distributed WPC network, or other similar wireless powered communication networks.

APPENDIX A

PROOF OF PROPOSITION 3.3

For both the upper and lower bounds, similar to the case of $M = 2$, we apply a 3-state Markov chain with state space $\{0, 1, 2\}$ with states 0, 1 and 2 denoting the battery power level of 0, in the range $[\frac{1}{2}P_s, P_s)$, and equal to P_s , respectively.

First, consider the upper bound on p_t . Since the harvested power in the region $a(X, h_2, r_h)$ is assumed to be equal to $\frac{1}{2}P_s$, it is easy to see that the state transition-probability matrix for this case is given by

$$\mathbf{P}^{(u)} = \begin{bmatrix} 1 - p_h & p'_2 + p_3 & p_1 \\ 0 & 1 - p_h & p_h \\ p_g & 0 & 1 - p_g \end{bmatrix}. \quad (56)$$

Let $\boldsymbol{\pi}^{(u)} = [\pi_0^{(u)}, \pi_1^{(u)}, \pi_2^{(u)}]$ denote the steady-state probability vector in this case. Solving $\boldsymbol{\pi}^{(u)}\mathbf{P}^{(u)} = \boldsymbol{\pi}^{(u)}$, we obtain $\pi_2^{(u)} = \frac{p_h}{p_h + p_g \left(1 + \frac{p'_2 + p_3}{p_h}\right)}$ and thus the upper bound on p_t can

be obtained by multiplying $\pi_2^{(u)}$ with p_g , according to (10).

Next, consider the lower bound on p_t . Since the harvested power in the region $a(X, h_2, r_h)$ is assumed to be 0, it is easy to obtain the state transition-probability matrix for this case as

$$\mathbf{P}^{(l)} = \begin{bmatrix} 1 - (p_1 + p'_2) & p'_2 & p_1 \\ 0 & 1 - (p_1 + p'_2) & p_1 + p'_2 \\ p_g & 0 & 1 - p_g \end{bmatrix}. \quad (57)$$

Similarly to the derivation of the upper bound on p_t , the lower bound on p_t can be found by finding the corresponding steady-state probability $\pi_2^{(l)} = \frac{p_1 + p'_2}{(p_1 + p'_2) + p_g \left(1 + \frac{p'_2}{p_1 + p'_2}\right)}$, and

then multiplying it with p_g . The proof of Proposition 3.3 is thus completed.

APPENDIX B

PROOF OF LEMMA 4.1

For convenience, we derive the non-outage probability $1 - P_{\text{out}}^{(p)}$ as follows with $P_{\text{out}}^{(p)}$ given in (28).

$$1 - P_{\text{out}}^{(p)} = \Pr \left\{ \frac{g_p P_p d_p^\alpha}{I_p + I_s + \sigma^2} \geq \theta_p \right\} \quad (58)$$

$$= \Pr \left\{ g_p \geq \frac{\theta_p d_p^\alpha}{P_p} (I_p + I_s + \sigma^2) \right\} \quad (59)$$

$$= \mathbb{E}_{I_p} \left[\mathbb{E}_{I_s} \left[\exp \left(-\frac{\theta_p d_p^\alpha}{P_p} (I_p + I_s + \sigma^2) \right) \right] \right] \quad (60)$$

$$= \exp \left(-\frac{\theta_p d_p^\alpha}{P_p} \sigma^2 \right) \mathbb{E}_{I_p} \left[\exp \left(-\frac{\theta_p d_p^\alpha}{P_p} I_p \right) \right] \mathbb{E}_{I_s} \left[\exp \left(-\frac{\theta_p d_p^\alpha}{P_p} I_s \right) \right], \quad (61)$$

where in (61), the expectations are separated since I_p and I_s are assumed to be independent as a result of Assumption 1. Note that $\mathbb{E}_{I_p} \left[\exp \left(-\frac{\theta_p d_p^\alpha}{P_p} I_p \right) \right]$ and $\mathbb{E}_{I_s} \left[\exp \left(-\frac{\theta_p d_p^\alpha}{P_p} I_s \right) \right]$ are Laplace transforms in terms of the random variables I_p and I_s , respectively, both with input parameter $\frac{\theta_p d_p^\alpha}{P_p}$. According to the result in [26, 3.21], the Laplace transform of the shot-noise process of an HPPP $\Lambda(\lambda)$ with density $\lambda > 0$, denoted by $I = \sum_{T \in \Lambda(\lambda)} g_T P |T|^{-\alpha}$, with input parameter s is given by

$$\mathbb{E}_I [\exp(-sI)] = \exp(-(Ps)^\frac{2}{\alpha} \lambda \varphi), \quad (62)$$

where $\{g_T\}_{T \in \Lambda(\lambda)}$ is a set of i.i.d. exponential random variables with mean 1, and φ is given in Lemma 4.1. Using (62), we can easily obtain $\mathbb{E}_{I_p} \left[\exp \left(-\frac{\theta_p d_p^\alpha}{P_p} I_p \right) \right]$ and

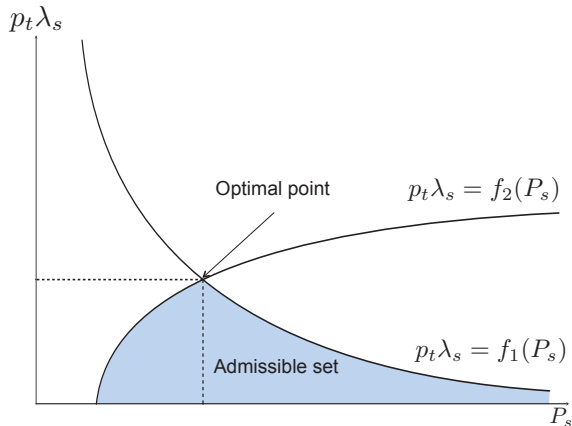


Fig. 17. Illustration of the optimal solution for Problem (P1).

$E_{I_s} \left[\exp \left(-\frac{\theta_p d_p^\alpha}{P_p} I_s \right) \right]$ and by substituting them to (61), the proof of Lemma 4.1 is thus completed.

APPENDIX C

PROOF OF LEMMA 4.2

The term $\Pr \left\{ \frac{g_s P_s d_s^{-\alpha}}{I_p + I_s + \sigma^2} < \theta_s \right\}$ in (32) is obtained by following the similar procedure in the proof of Lemma 4.1, given by

$$\Pr \left\{ \frac{g_s P_s d_s^{-\alpha}}{I_p + I_s + \sigma^2} < \theta_s \right\} = 1 - \exp(-\tau_s), \quad (63)$$

where τ_s is given in (34).

Next, under the assumption $P_p \gg P_s$, it is reasonable to assume that the interference from even only one single PT inside $b(Y_o, r_g)$ is sufficient to cause an outage to the typical SR at the origin. Consequently, we have $\Pr \left\{ \frac{g_s P_s d_s^{-\alpha}}{I_p + I_s + \sigma^2} < \theta_s \mid \bar{\mathcal{E}} \right\} \approx 1$. Substituting this result, (63) and $\Pr\{\mathcal{E}\} = e^{-\pi r_g^2 \lambda_p} = 1 - p_g$ into (32) yields (33). The proof of Lemma 4.2 is thus completed.

APPENDIX D

PROOF OF THEOREM 5.1

From (30) and (34), the constraints $\tau_p \leq \mu_p$ and $\tau_s \leq \mu_s$ given in (39) and (40) are equivalent to $p_t(P_s)\lambda_s \leq f_1(P_s)$ and $p_t(P_s)\lambda_s \leq f_2(P_s)$, respectively, where

$$f_1(P_s) = \left[\frac{1}{\theta_p^\alpha d_p^2 \varphi} \left(\mu_p - \frac{\theta_p d_p^\alpha \sigma^2}{P_p} \right) - \lambda_p \right] \left(\frac{P_s}{P_p} \right)^{-\frac{2}{\alpha}}, \quad (64)$$

$$f_2(P_s) = \frac{1}{\theta_s^\alpha d_s^2 \varphi} \left(\mu_s - \frac{\theta_s d_s^\alpha \sigma^2}{P_s} \right) - \lambda_p \left(\frac{P_s}{P_p} \right)^{-\frac{2}{\alpha}}. \quad (65)$$

As illustrated in Fig. 17, $f_1(P_s)$ decreases whereas $f_2(P_s)$ increases with growing P_s . The shaded region in Fig. 17 shows the admissible set of $(P_s, p_t \lambda_s)$ that satisfies the given outage probability constraints. It is observed that the optimal value of $p_t(P_s)\lambda_s$ is the intersection of the two curves $p_t(P_s)\lambda_s = f_1(P_s)$ and $p_t(P_s)\lambda_s = f_2(P_s)$. The intersection point can

be found by solving $f_1(P_s) = f_2(P_s)$, which has no closed-form solution in general with $\sigma^2 > 0$. However, by letting $\sigma^2 = 0$, the closed-form solution of P_s^* can be obtained as $\frac{\theta_s}{\theta_p} \left(\frac{d_s}{d_p} \right)^\alpha \left(\frac{\mu_s}{\mu_p} \right)^{-\frac{\alpha}{2}} P_p$. From $p_t(P_s^*)\lambda_s^* = f_1(P_s^*)$ and (64),

we then obtain $p_t(P_s^*)\lambda_s^* = \frac{\mu_s(\mu_p - \varphi \theta_p^\alpha d_p^2 \lambda_p)}{\theta_s^\alpha d_s^2 \mu_p \varphi}$, and accordingly

$$\lambda_s^* = \frac{\mu_s(\mu_p - \varphi \theta_p^\alpha d_p^2 \lambda_p)}{p_t(P_s^*) \theta_s^\alpha d_s^2 \mu_p \varphi}. \quad \text{Theorem 5.1 is thus proved.}$$

REFERENCES

- [1] T. Le, K. Mayaram, and T. Fiez, "Efficient far-field radio frequency energy harvesting for passively powered sensor networks," *IEEE J. Solid-State Circuits*, vol. 43, no. 5, pp. 1287-1302, May 2008.
- [2] A. M. Zungeru, L. M. Ang, S. Prabaharan, and K. P. Seng, "Radio frequency energy harvesting and management for wireless sensor networks," *Green Mobile Devices and Netw.: Energy Opt. Scav. Tech.*, CRC Press, pp. 341-368, 2012.
- [3] R. J. M. Vullers, R. V. Schaijk, I. Doms, C. V. Hoof, and R. Mertens, "Micropower energy harvesting," *Elsevier Solid-State Circuits*, vol. 53, no. 7, pp. 684-693, July 2009.
- [4] D. Bouchouicha, F. Dupont, M. Latrach, and L. Ventura, "Ambient RF energy harvesting," *Int. Conf. Renew. Energies and Power Qual. (ICREPO)*, Mar. 2010.
- [5] T. Paing, J. Shon, R. Zane, and Z. Popovic, "Resistor emulation approach to low-power RF energy harvesting," *IEEE Trans. Power Elect.*, vol. 23, no. 3, pp. 1494-1501, May 2008.
- [6] H. Jabbar, Y. S. Song, and T. T. Jeong, "RF energy harvesting system and circuits for charging of mobile devices," *IEEE Trans. Consumer Elect.*, vol. 56, no. 1, pp. 247-253, Feb. 2010.
- [7] C. K. Ho and R. Zhang, "Optimal energy allocation for wireless communications with energy harvesting constraints," *IEEE Trans. Sig. Process.*, vol. 60, no. 9, pp. 4808-4818, Sep. 2012.
- [8] O. Ozel, K. Tutuncoglu, J. Yang, S. Ulukus, and A. Yener, "Transmission with energy harvesting nodes in fading wireless channels: optimal policies," *IEEE J. Sel. Areas Commun.*, vol. 29, no. 8, pp.1732-1743, Sep. 2011.
- [9] K. Huang, "Spatial throughput of mobile ad hoc networks with energy harvesting," to appear in *IEEE Trans. Inf. Theory (Available on-line at http://arxiv.org/abs/1111.5799)*.
- [10] D. Niyato, E. Hossain, and A. Fallahi, "Sleep and wakeup strategies in solar-powered wireless sensor/mesh networks: performance analysis and optimization," *IEEE Trans. Mobile Computing*, vol. 6, no. 2, pp. 221-236, Feb. 2007.
- [11] W. C. Brown, "The history of power transmission by radio waves," *IEEE Trans. Microwave Theory and Tech.*, vol. 32, pp. 1230-1242, Sep. 1984.
- [12] L. R. Varshney, "Transporting information and energy simultaneously," in *Proc. IEEE Int. Symp. Inf. Theory (ISIT)*, pp. 1612-1616, July 2008.
- [13] P. Grover and A. Sahai, "Shannon meets Tesla: wireless information and power transfer," in *Proc. IEEE Int. Symp. Inf. Theory (ISIT)*, pp. 2363-2367, June 2010.
- [14] R. Zhang and C. K. Ho, "MIMO broadcasting for simultaneous wireless information and power transfer," *IEEE Trans. Wireless Commun.*, vol. 12, no. 5, pp. 1989-2001, May 2013.
- [15] X. Zhou, R. Zhang, and C. K. Ho, "Wireless information and power transfer: architecture design and rate-energy tradeoff," *submitted to IEEE Trans. Commun. (Available on-line at http://arxiv.org/abs/1205.0618)*
- [16] L. Liu, R. Zhang, and K. C. Chua, "Wireless information transfer with opportunistic energy harvesting," *IEEE Trans. Wireless Commun.*, vol. 12, no. 1, pp. 288-300, Jan. 2013.
- [17] K. Huang and V. K. N. Lau, "Enabling wireless power transfer in cellular networks: architecture, modeling and deployment," *submitted for publication. (Available on-line at http://arxiv.org/abs/1207.5640)*
- [18] S. Haykin, "Cognitive radio: brain-empowered wireless communications," *IEEE J. Sel. Areas Commun.*, vol. 23, no. 2, pp. 201-220, Feb. 2005.
- [19] Q. Zhao and B. M. Sadler, "A survey of dynamic spectrum access," *IEEE Sig. Process. Mag.*, vol. 24, no. 3, pp. 79-89, May 2007.
- [20] R. Zhang, Y. C. Liang, and S. Cui, "Dynamic resource allocation in cognitive radio networks," *IEEE Sig. Process. Mag.*, vol. 27, no. 3, pp. 102-114, May 2010.

- [21] C. Yin, L. Gao, and S. Cui, "Scaling laws for overlaid wireless networks: a cognitive radio network versus a primary network," *IEEE/ACM Trans. Netw.*, vol. 18, no. 4, pp. 1317-1329, Aug. 2010.
- [22] K. Huang, V. K. N. Lau, and Y. Chen, "Spectrum sharing between cellular and mobile ad hoc networks: transmission-capacity trade-off," *IEEE J. Sel. Areas Commun.*, vol. 27, no. 7, pp. 1256-1267, Sep. 2009.
- [23] J. Lee, J. G. Andrews, and D. Hong, "Spectrum sharing transmission capacity," *IEEE Trans. Wireless Commun.*, vol. 10, no. 9, pp. 3053-3063, Sep. 2011.
- [24] C. H. Lee and M. Haenggi, "Interference and outage in Poisson cognitive networks," *IEEE Trans. Wireless Commun.*, vol. 11, no. 4, pp. 1392-1401, Apr. 2012.
- [25] L. Xie, Y. Shi, Y. T. Hou, and H. D. Sherali, "Making sensor networks immortal: an energy-renewal approach with wireless power transfer," *IEEE/ACM Trans. Netw.*, vol. 20, no. 6, pp. 1748-1761, Dec. 2012.
- [26] M. Haenggi and R. K. Ganti, "Interference in large wireless networks," *Found. Trends in Netw.*, NOW Publishers, vol. 3, no. 2, pp. 127-248, 2008.
- [27] S. Weber and J. G. Andrews, "Transmission capacity of wireless networks," *Found. Trends in Netw.*, NOW Publishers, vol. 5, no. 2-3, pp. 109-281, 2012.
- [28] J. F. C. Kingman, *Poisson processes*. Oxford University Press, 1993.